

# The 2006 Interferometry Imaging Beauty Contest

Peter R. Lawson<sup>1</sup>, William D. Cotton<sup>2</sup>, and Christian A. Hummel<sup>3</sup>  
Michael Ireland<sup>4</sup>, John D. Monnier<sup>5</sup>,  
Eric Thiébaud<sup>6</sup>, Sridharan Rengaswamy<sup>9</sup>  
Fabien Baron<sup>7</sup>, John S. Young<sup>7</sup>,  
Stefan Kraus<sup>8</sup>, Karl-Heinz Hoffman<sup>8</sup>, Gerd P. Weigelt<sup>8</sup>  
Olivier Chesneau<sup>10</sup>

<sup>1</sup>Jet Propulsion Laboratory, California Institute of Technology, Pasadena, CA, USA

<sup>2</sup>National Radio Astronomy Observatory, Charlottesville, VA, USA

<sup>3</sup>European Southern Observatory, Santiago, Chile

<sup>4</sup>California Institute of Technology, Pasadena, CA, USA

<sup>5</sup>University of Michigan, Ann Arbor, MI, USA

<sup>6</sup>Astrophysics Group, Cavendish Laboratory, Cambridge, United Kingdom

<sup>7</sup>CRAL / Observatoire de Lyon, Saint Genis Laval, France

<sup>8</sup>Max Planck Institute for Radio Astronomy, Bonn, Germany

<sup>9</sup>Space Telescope Science Institute, Baltimore, MD, USA

<sup>10</sup>Observatoire de la Côte d'Azur, France

## ABSTRACT

We present a formal comparison of the performance of algorithms used for synthesis imaging with optical/infrared long-baseline interferometers. Five different algorithms are evaluated based on their performance with simulated test data. Each set of test data is formatted in the OI-FITS format. The data are calibrated power spectra and bispectra measured with an array intended to be typical of existing imaging interferometers. The strengths and limitations of each algorithm are discussed.

**Keywords:** Astronomical software, closure phase, aperture synthesis, imaging, optical, infrared, interferometry

## 1. INTRODUCTION

The 2006 Interferometry Imaging Beauty Contest is the second in what will likely be a series of imaging contests, held to promote the development of imaging algorithms that are specifically tailored to long-baseline optical/infrared data. Interferometers that operate at optical or infrared wavelengths are subject to the noise introduced by atmospheric turbulence; the phase information that they record at each baseline is meaningless, because it contains many cycles of phase due to the randomly varying index of refraction in the atmosphere above each telescope. Optical/infrared interferometers that are designed for imaging must make measurements of phases using three or more baselines simultaneously. If the baselines form a geometrical pattern that is closed, such as a triangle or rectangle, then the *sum* of all the phases recorded around those baselines is independent of the atmospheric phase at each telescope and instead depends only on the geometry of the source. Imaging interferometers typically measure visibility-squared on each baseline and closure phases around the baselines of triplets of telescopes.

Imaging with optical/infrared interferometers is still relatively new, having been pioneered with long-baseline arrays in 1995.<sup>1</sup> Up until 2004 only three interferometers (COAST, NPOI, and IOTA) had the ability to record closure phases. Since then three more interferometers (ISI, CHARA, VLTI/AMBER), have begun imaging.

---

Further author information: Send correspondence to Peter Lawson, Jet Propulsion Laboratory, MS 301-451, 4800 Oak Grove Drive, Pasadena, CA 91109-8099, USA. E-mail: Peter.R.Lawson@@jpl.nasa.gov; Telephone: +1 (818) 354-0747.

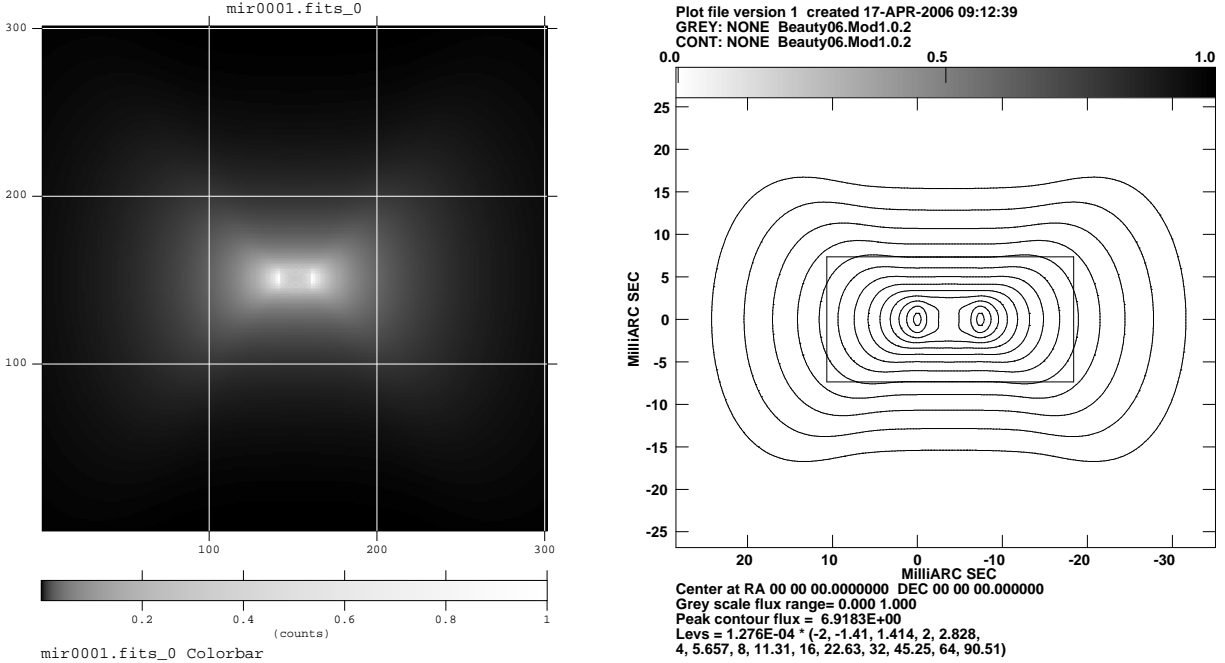


**Figure 1.** Model for the contest data. The model is shown in greyscale (left) and as a contour plot (right). The contour levels are multiples of  $1.276 \times 10^{-4}$ , where the factors are -2, -1.41, 1.41, 2.0, 2.828, 4.0, 5.657, 8, 11.31, 16.0, 22.63, 32.0, 45.25, 64.0, 90.51. The image is a  $301 \times 301$  (0.35 mas) pixel image. The contest data was produced from this image through simulations that sampled the source by a 3-beam VLTI/AMBER beam combiner.

Science results from these efforts have been primarily limited to binary star observations, limb-darkening of stars, and more recently measurements of Young Stellar Objects. Most reported astrophysical results from optical/infrared interferometers continue to be made with single-baseline observations. Imaging with long-baseline interferometers at optical and infrared wavelengths is still a maturing field.

Beginning in 2001, the International Astronomical Union’s Working Group on Optical/Infrared Interferometry encouraged the development of a common format for calibrated imaging data. As a result the Optical Interferometry Exchange Format (OI-FITS) was released in 2003 and published in the refereed literature in 2005.<sup>2</sup> In parallel with that work, and involving many of the same principals, the first Imaging Beauty Contest was organized in 2004.<sup>3</sup> There were several motivations for the imaging beauty contest: (1) Encourage the use of the OI Exchange Format, identify problems in its definition, and revise it as necessary; (2) Engage the interferometry community in a formal assessment of existing software; (3) Encourage the development of new software tailored to the needs of optical interferometry. In each of these areas the contests have proven very useful. The contests have been well received by the community and so are likely to remain a staple of the SPIE interferometry meetings for years to come. Although it has proven difficult to pose the contest in a way that answers a specific question, it can be clearly seen by the results that most approaches to imaging are indeed successful.

### 1.1. Choice of Contest Data

The 2004 contest had modeled two bright objects observed with the Navy Prototype Optical Interferometer using a six-telescope configuration. Several contestants (Serge Meimon in particular) felt that the 2006 contest should provide a more challenging subject, being a more resolved source observed with a sparser array. These guidelines were then adopted.

The contest image was a semi-realistic optically thin disk model, mir0001.fits, provided to Christian Hummel by Olivier Chesneau. The model is shown in Fig. 1. Christian simulated 4 nights of full earth-rotation aperture

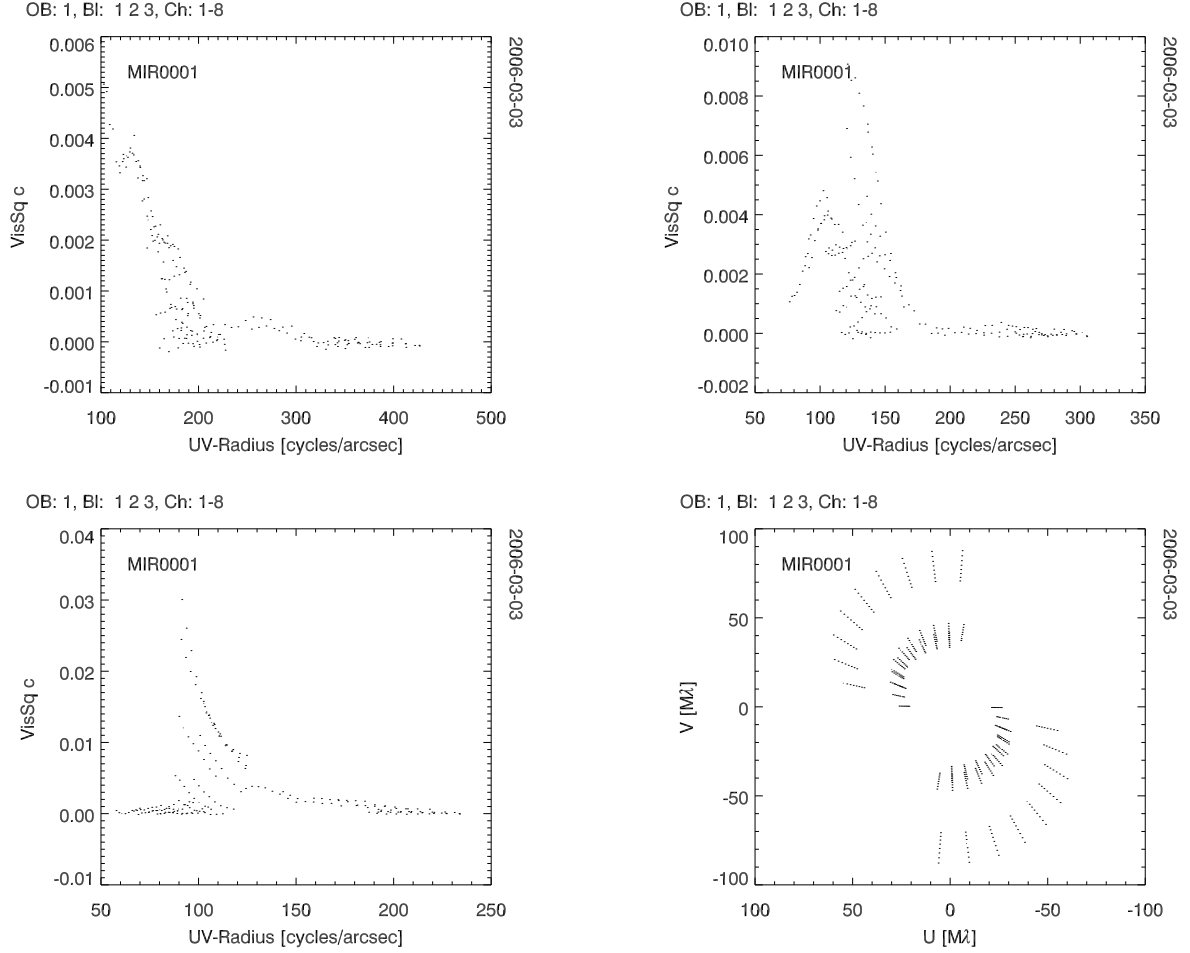


**Figure 2.** Visibilities-squared and  $(u, v)$  coverage for the model data.

synthesis with the VLTI’s AMBER beam-combiner in low-resolution J, H, and K mode. The 8-m Unit Telescopes were used for the simulations, with station combinations (1,2,3), (1,2,4), (1,3,4), and (2,3,4). Christian adjusted the noise so that there was some useful signal on the longest baselines despite the horribly small visibility (squared) amplitudes. All UT combinations were used since single combinations appeared to have little chance of mapping the disk structure. Christian considered this model as really difficult, given the extended flux and the sharp featured at the inner disk rim. The extended emission was reduced to below 1% of peak to keep the simulation from running too long.

There are several reasons why this model is however unrealistic: 1) There is no correlated noise in the data. It proved too difficult to model for this contest; 2) There is no wavelength dependence to the source structure, even though J, H, and K-band data is provided; 3) The visibility amplitudes are so low, it might prove impossible to fringe track on such an object; 4) The European Southern Observatory would be unlikely to ever allocate four full nights — using all four 8-m telescopes — for Earth-rotation aperture synthesis on this object.

The contest data sets were provided in the OI-FITS format. This obliged contestants to work with this data format before using the data in their programs. Test data were provided as a preliminary to the contest itself. This allowed contestants to see if their software could reproduce a simple image — in this case a binary star with a given separation, magnitude difference, and orientation. Data from the 2004 was also available as a further check. The contest data were then presented without any information as to what they represented to provide a

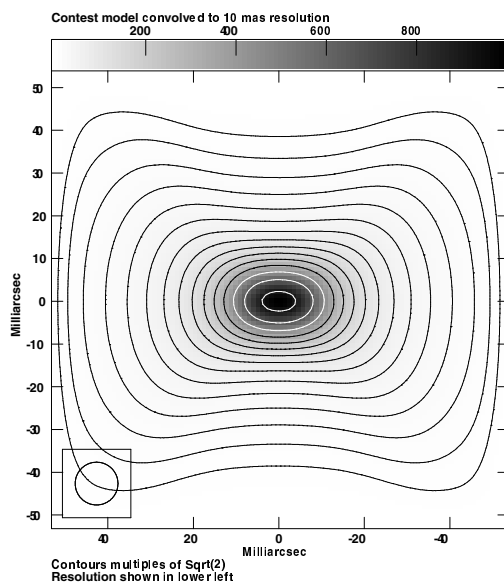


**Figure 3.** The Clue.

blind test. As part of the contest the participants were asked not only to produce images, but to interpret in the images what they believed to be true features and what they believed were artifacts of the imaging process. Deadlines were imposed to provide a consistent schedule compatible with the timetable of the conference.

The contest data files for each night of observation were `2006-03-03.fits`, `2006-03-04.fits`, `2006-03-05.fits`, and `2006-03-06.fits`. These files were made available to the contestants, and are available to interested readers, at the website of the IAU Working Group, hosted through the Optical Long Baseline Interferometry News <http://olbin.jpl.nasa.gov/iau/2006/beauty.html>.

## 1.2. The Clue

However, many participants voiced the objection that the object was far too difficult, the source visibilities were far too low, and the object was very poorly constrained by the data. As a group, the contestants requested further information about the source. In response, William Cotton provided a FITS format image of the model convolved to a resolution of 10 mas. This provided the overall shape of the extended emission, without revealing the nature of the central source. The clue is shown in Fig. 3. After providing this additional information, there were additional request for clarification, but these requests were denied by the organizers.

## 1.3. Submission Guidelines

The contestants were requested to provide their submissions in a standard format. Submissions to the contest consisted of simple FITS images with the following descriptive information provided either in the FITS image header or separately:

1. Pixel separation and orientation as well as any rotation and/or skew.
2. Pixel brightness units: e.g. Flux density per pixel or flux density per resolution element and in the latter case the equivalent number of pixels per resolution element.
3. Description of resolution in image including any convolution.
4. Cell spacing provided either in the FITS header or separately.
5. Discussion of which features were considered real.
6. A visual representation of the image (contour, greyscale, etc.) could also have been submitted but the entry will be judged on the FITS image alone.

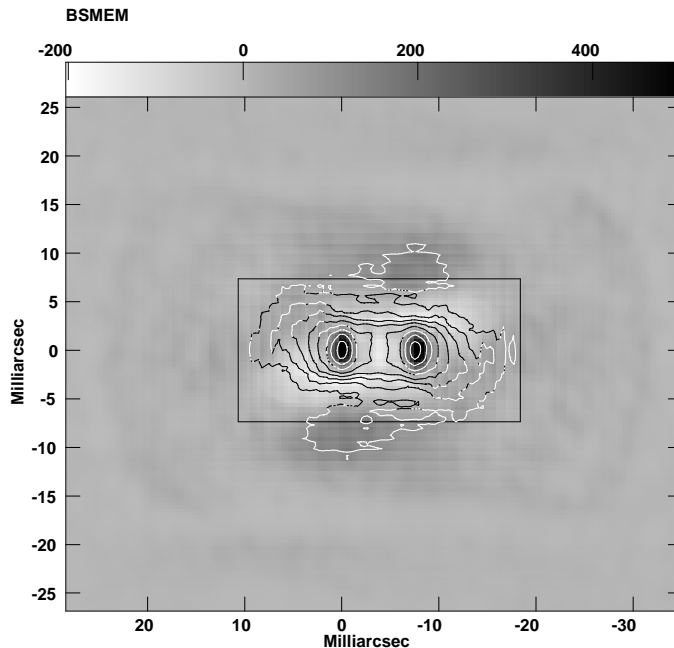


**Figure 4.** Entry for BSMEM.

Additional text was requested from each contestant to briefly describe the software and its advantages. This text was edited and included in the present paper. The results and presentations now follow.

## 2. BSMEM

FABIEN BARON AND J. S. YOUNG (UNIVERSITY OF CAMBRIDGE)

Our software package, BSMEM (BiSpectrum Maximum Entropy Method),<sup>4</sup> has already been introduced in the former SPIE proceeding for the Interferometry Beauty Contest 2004. It uses a fully Bayesian approach to the image reconstruction problem, by maximizing the posterior probability of the reconstructed image given the input data set. As BSMEM independently exploits the power spectrum points, the triple product amplitudes, and the phase closures, it can handle all types of data sparseness (such as the frequent case of missing closures). Current work on BSMEM involves further testing of its behavior on difficult data sets : with poor uv coverage, poor SNR, missing bispectrum or powerspectrum points, etc. BSMEM reconstruction can be model independent, meaning a flat prior is used, or can take advantage of a user-made starting model.

Our submitted image is 512 x 512 pixels, and the pixel separation is 0.2 mas. No convolution has been applied. The image is shown in Fig. 4. The total flux in the image is renormalized by BSMEM (and so equal to 1.00). The contour plot is at 12

In the absence of any information about the observed object, we have first used one of our default models, a centered broad Gaussian (30 mas FWHM), treated as a pixel-weighting by BSMEM. This first reconstruction has allowed us to determine the correct field of view and to identify what we believe to be the main features : two compact disk-shaped components separated by 8 mas and a wider diffuse background about 30 mas in diameter. At least some basic knowledge on the nature of the sources would have been useful to decide which starting model to use as a basis for further reconstructions. The important errors on the bispectrum data imply that our image is too symmetric. Another problem arises as the data are not very constraining : a wrong model could easily introduce artifacts into the reconstructed image, due to excessive bias from pixel-weighting. We have indeed tried without success to improve our first image by choosing to put an emphasis on the two compact objects. While the resulting image shows ring-like shapes around both objects, we could not be certain whether those features were real ones or model introduced artifacts. So we have actually decided to reject this image and consequently we have submitted the previous one.

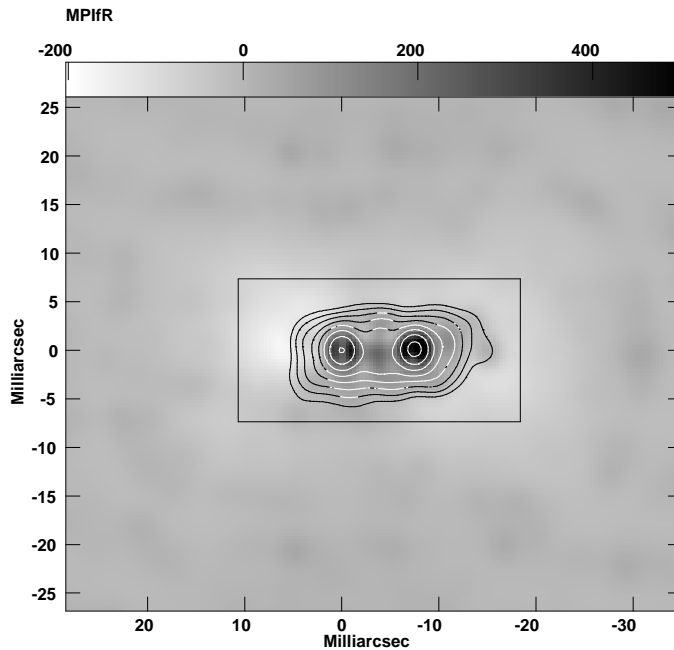


**Figure 5.** Entry for Building Block Method.

### 3. BUILDING BLOCK METHOD

STEFAN KRAUS, KARL-HEINZ HOFFMAN,  
GERD WEIGELT (MAX PLANCK INSTITUTE FOR RADIO ASTRONOMY)

The Building Block method<sup>5</sup> was developed to reconstruct diffraction-limited images from the object bispectrum obtained with speckle or long-baseline interferometry.

As the intensity distribution of an object can also be described as a sum of many components, our algorithm reconstructs images iteratively by adding *building blocks* (e.g.  $\delta$ -functions) to a model image. The initial model image may simply consist of a single  $\delta$  peak, to which components are added. Within each iteration step, the next building block is positioned at the particular coordinate which leads to an image which minimizes the deviations between the model bispectrum and the measure object bispectrum. Beside positive building blocks, which are added at the position of the absolute minimum of the distance function, building blocks can also be subtracted at the position of the absolute maximum. Experience shows, that adding positive and negative building blocks simultaneously improves the converge of the algorithm, when the positivity constraint for the final image is taken into account.

The contest entry imaged with the Building Block Method is shown in Fig. 5. The reconstruction submitted was performed without regularization.

### 4. MARKOV CHAIN IMAGER (MACIM)

MICHAEL IRELAND (CALIFORNIA INSTITUTE OF TECHNOLOGY)

The MACIM (MARkov Chain IMager) algorithm<sup>6</sup> was used for this contest entry. The algorithm has several advantages:

1. The best region of image is found by a simulated annealing algorithm. This means that it is unlikely to get ‘stuck’ in a local chi-squared minimum.
2. The way in which flux elements are moved around creates a natural maximum entropy-like regularization.
3. The algorithm can output not only a single image, but a set of images consistent with the data (Markov Chains of images). This enables the possibility of statistics on the range of output images.

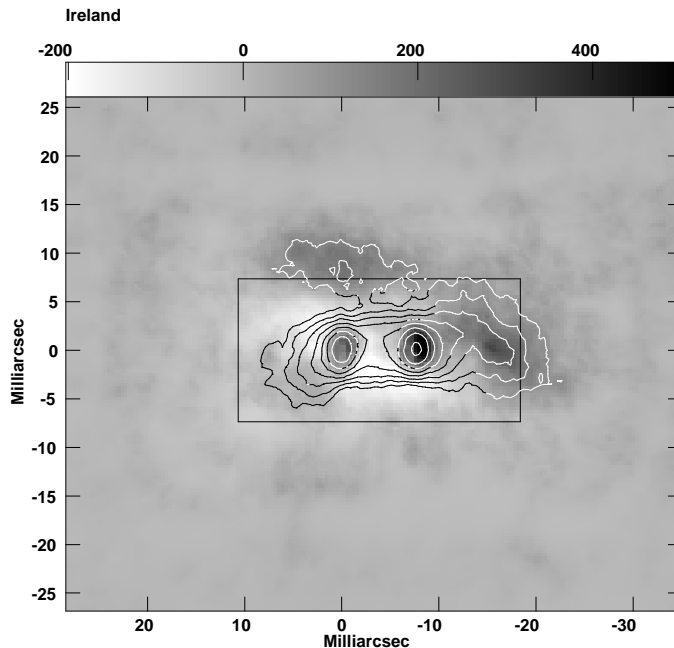


**Figure 6.** Entry for Markov Chain Imager.

4. The lack of derivatives in the algorithm mean that novel regularization techniques can be used (not used for this data set, because of the extended emission).

The contest entry image shown in Fig. 6 has a scale of 0.2 mas per pixel (501 pixels across), as defined by the fits keywords NAXIS1 and SCALE. The total brightness of the image sums to 1.0 - so this is flux density per pixel. The image has a natural resolution of about 1.0 mas (i.e. this would be the FWHM of a high S/N point source with the settings I used: standard deviation half of this). Note that this isn't the raw software output, which is naturally noisy, but has 2D Voroni binning applied to reduce the apparent noise of the lowest contrast features ('triangular' patterns at 1Given that even the natural noise in the software was at the 1flux level, I certainly wouldn't believe anything at this level.

In the process of finding this image, the software found several other images that looked slightly different with chi-squared of 1. They all had the binary at the image centre and extended emission with straight horizontal features above and below the binary. Ordinarily, I wouldn't trust any other features in the image, but given the field-of-view constraint, I find it likely that the excess emission to the North of the Eastern component of the binary and to the West of the Western component of the binary are also real. However, the sidedness of the image is not constrained by the data - e.g. the excess emission to the West of the Western component could be to the East of the Eastern component and still give a chi-squared of 1 with similar entropy.

## 5. MIRA

ERIC THIÉBAUT (CRAL / OBSERVATOIRE DE LYON)

MIRA (Multi-aperture Image Reconstruction Algorithm) is an image reconstruction algorithm designed to deal with optical interferometric data.<sup>7</sup> The development of MIRA was supported by the JMMC (Jean-Marie Mariotti Center).

MIRA implement mainy different kind of regularization terms (Tikhonov,  $\ell_2 - \ell_1$  smoothness penalization, maximum entropy, etc). The idea being that regularization is required to cope with missing data, the user of MIRA is encouraged to try different kinds of regularization and to figure out the incidence of the choice of the particular a priori onto the recovered image.

For the *Interferometry Imaging Beauty Contest*, low frequency data were completely missing and the highest measured squared visibility was  $\sim 3\%$ . Therefore, the high frequency structures must have a very low contrast whereas the low resolution shape of the object is not accessible from the interferometric data alone. Owing to

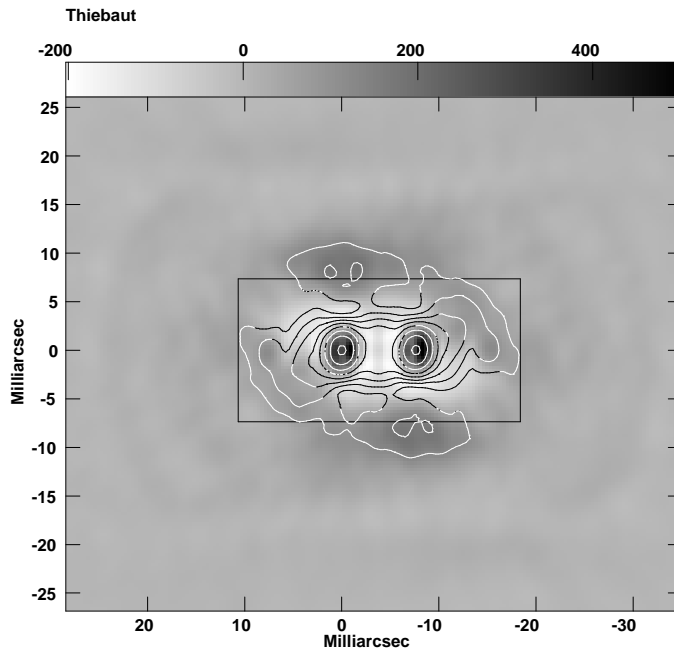


**Figure 7.** Entry for MIRA.

the high contrast and to the large low frequency vacuum in the *Interferometry Imaging Beauty Contest* data set, a regularization able to interpolate the low frequency gap has to be used. For these reasons, the following quadratic regularization was chosen:

$$f_{\text{prior}}(\mathbf{x}) = \sum_{j,k} w_{j,k} x_{j,k}^2 \quad (1)$$

where the regularization weights  $w_{j,k}$  were chosen so as to achieve spectral smoothing, *i.e.*:

$$f_{\text{prior}}(\mathbf{x}) = \sum_{j,k} w_{j,k} x_{j,k}^2 \simeq \sum_{u,v} |\hat{x}_{u+1,v} - \hat{x}_{u,v}|^2 + \sum_{u,v} |\hat{x}_{u,v+1} - \hat{x}_{u,v}|^2$$

where  $\hat{x}_{u,v}$  is the discrete Fourier transform of the discretized image  $x_{j,k}$ . This kind of regularization enforces smoothness of the Fourier spectrum of the image and, accordingly, it enforces compactness of the brightness distribution in the field of view.

During the reconstruction, the strength of regularization must be tuned. This was done by monitoring the statistics of the residuals. The rule of thumb is as follows:

1. if the residuals are significantly greater (on average) than the standard deviations, then the regularization level is too high and must be reduced to account for meaningful information from the data;
2. if the residuals are significantly smaller (on average) than the standard deviations, then the model is too good to be true and regularization must be strengthened to avoid fitting features due to the noise.

The low resolution image (*clue.10.fits*) was used to set the size of the synthesized field of view which is  $\simeq 105$  milliarcsecond. The highest spatial frequency requires a spatial sampling size of at least  $\simeq 0.88$  milliarcseconds however since the squared visibilities drop to zero before this limit, we used the same pixel size as in the low resolution image, *i.e.*  $\simeq 1.05$  milliarcseconds.

Since most of phase closures are compatible with a symmetrical object ( $\beta_k \simeq 0$  or  $\beta_k \simeq \pm\pi$ ), the algorithm was started with a symmetrical initial image and run without accounting for the phase closures until the residuals of the squared visibilities were statistically well fitted. During this first stage, the object was constrained to be symmetrical and the level of regularization was slowly decreased as described above. Then, the phase closure data were introduced and the algorithm continued.

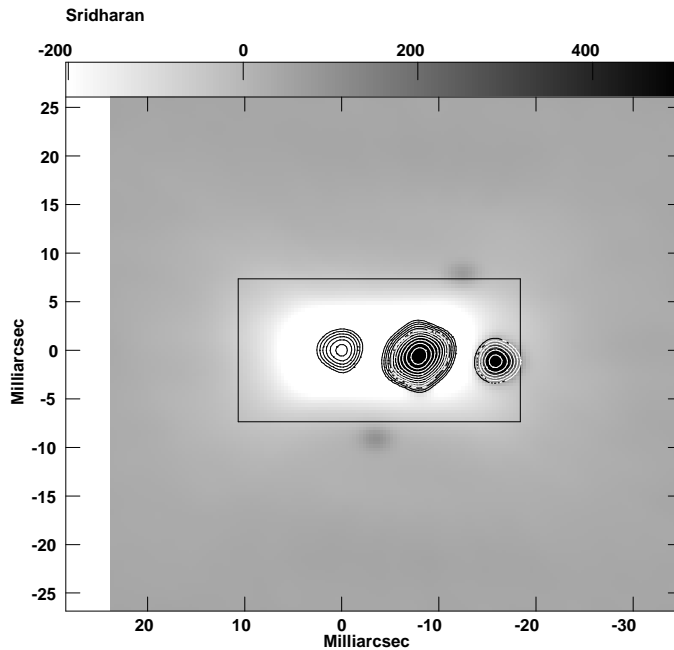


**Figure 8.** Entry for Recursive Phase Reconstruction.

The final result, shown in Fig. 7, is convolved with a Gaussian of FWHM=10 milliarcseconds and was compared qualitatively to the low resolution image (*clue.10.fits*) to assert that its low resolution part was properly recovered.

In the restored image radial rays can be seen at very low contrast, these features correspond to the directions of sampling in the  $(u, v)$  plane and are certainly artifacts. Because the squared visibilities become compatible with zero after  $\sim 7 \times 10^7$  cycle $^{-1}$ , the object has no significant details smaller than 2–3 milliseconds; the restored image would therefore benefit from an additional regularization term aimed at image (not spectrum) smoothness which could wipe out some of the small structures far from the center of the field of view. Finally we observed that the residuals of many phase closures in the middle frequency range are much worse than the other residuals. This is either an indication that some features are missing from the result or this the signature of some of the above mentioned artifacts.

## 6. RECURSIVE PHASE RECONSTRUCTION

SRIDHARAN RENGASWAMY (SPACE TELESCOPE SCIENCE INSTITUTE)

The recursive phase reconstruction procedure for estimating the Fourier phases was borrowed from the speckle code developed by me earlier and a new software, that would do the rest of the processing was developed. The software is still in a nascent stage.

In fact, I tried out two different implementations of phase reconstruction, a recursive phase reconstruction that does not make use of 50% of the bispectrum values and Singular Value Decomposition (SVD) meethod that makes use of all the observed bispectrum values, and both of them yield consistent maps but they not necessarily ensure that the restored Fouries phases are reliable.

1. The squared visibility amplitudes and the bispectrum phases were weighed by a factor  $\beta = \text{SNR}/(\text{SNR}+1)$ , where SNR is the respective signal-to-noise ratio.
2. The product of the square root of the squared visibilities and the estimated phases was Fourier inverted to get the "dirty map" or the restored image.
3. The restored images were cleaned by 50 iterations of standard CLEAN, with a loop gain of 0.1.

4. The aforesaid procedure was repeated for each data set, and the CLEANed maps were averaged to obtain the final map.
5. The restored image shows a strong central source (at the center of the field of view) and two sources on either side of it along (almost) east-west direction. There are some faint extensions along the northern and southern sides.
6. I believe that (a) the central source and the two sources on either side of it along the east-west direction are real. (b) the tilt (approximately) along the east-west direction is real.

I think the morphology of the source is as follows: There is a bright central source (which gives rise to almost constant visibility even at the longest baseline) surrounded by a ring or a doughnut shaped source. As a whole the source is tilted close to edge-on view so that the source appears compressed in the north-south direction with more surface density per pixel compared to east-west direction. In the image, the source is resolved out in the east-west direction, the edges of the ring appear as two sources on either side.

## 7. RAPPORT SUR LE CONCOURS DE L'ANNÉE 2006

(COMMISSAIRES: MM. COTTON, HUMMEL, LAWSON RAPPORTEUR.)

William Cotton, the contest judge, processed the submitted entries according to the following steps to determine the contest winner.

1. The initial model was convolved with a 1 mas Gaussian and coordinates were labeled with 0.35 mas spacing and positions relative to the peak of the eastern component (in the convolved image)
2. The image coordinates were labeled with the spacing provided by the entry, and aligned on the peak of the eastern component.
3. Interpolating all images to the geometry of the model image.
4. Normalize all images (including model) by the sum of the pixel values inside the box defined by corners (110,130), (193,172) (1-relative, inclusive).
5. Subtract normalized model from each normalized entry and multiplied by 1.0e6
6. The quality measure is the RMS about zero of the difference image evaluated inside the normalization box.

All but one entry obtained the correct basic model and amongst these there was a relatively small range of quality measures.

**Table 1.** 2006 Imaging Beauty Contest Results

Entry	RMS
BSMEM	90.5
MIRA	97.2
Building Block Method	109.1
MACIM	114.7
Recursive Phase Reconstruction	885.73

For each entry two plot files are made, one in color and one in black and white which show contours of the entry after interpolated onto the same grid and normalized with greyscale or color showing the residuals from the model. All contours are the same are given on the model image and the range of residuals shown is the same for all entries.



**Figure 9.** The award ceremony for the 2006 Imaging Beauty Contest. The winner of the 2006 award was BSMEM. Fabien Baron, pictured in the center, is shown receiving the award on behalf of himself and John Young of the University of Cambridge. Two of the contest organizers, Peter Lawson (left) and Christian Hummel (right), are shown congratulating the winners.

The organizers of the contest, on behalf of the Scientific Organizing Committee of the IAU Working Group on Optical/IR Interferometry, are pleased to announce BSMEM as the winner of the 2006 Interferometry Imaging Beauty Contest.

The winning team, Fabien Baron and John Young, were presented with a certificate of their achievement on 29 May 2006 in front of the audience at the SPIE conference on *Advances in Stellar Interferometry* in Orlando, Florida, USA.

### ACKNOWLEDGMENTS

Work by PRL was carried out at the Jet Propulsion Laboratory, California Institute of Technology, under contract with the National Aeronautics and Space Administration. Work by WDC was supported by the National Radio Astronomy Observatory, a facility of the National Science Foundation operated under cooperative agreement by Associated Universities, Inc. The contest data and further information about the 2004 contest can be found at <http://olbin.jpl.nasa.gov/iau/2004/beauty.html>.

### REFERENCES

1. J. Baldwin, M. Beckett, R. Boysen, D. Burns, D. Buscher, G. Cox, C. Haniff, C. Mackay, N. S. Nightingale, J. Rogers, P. Scheuer, T. Scott, P. Tuthill, P. Warner, D. Wilson, and R. Wilson., "The first images from an optical aperture synthesis array: mapping of Capella with COAST at two epochs," *Astron. Astrophys.* **306**, pp. L13–L16, 1996.
2. T. A. Pauls, J. S. Young, W. D. Cotton, and J. Monnier, "Data exchange standard for optical (visible/IR) interferometry," *Pub. Astron. Soc. Pac.* **117**, pp. 1255–1262, 2005.

3. P. Lawson, W. Cotton, C. Hummel, J. Monnier, M. Zhao, J. Young, H. Thorsteinsson, S. Meimon, L. Mugnier, G. L. Besnerais, E. Thiebaut, and P. Tuthill, "An interferometry imaging beauty contest," in *New Frontiers in Stellar Interferometry*, W. A. Traub, ed., *Proc. SPIE* **5491**, pp. 886–899, 2004.
4. D. Buscher, "Direct maximum-entropy image reconstruction from the bispectrum," *Proc. IAU Symp.* **158**, pp. 91–93, 1994.
5. K. Hofmann and G. Weigelt, "Iterative image reconstruction from the bispectrum," *Astron. Astrophys.* **278**, pp. 328–339, 1993.
6. M. Ireland, J. D. Monnier, and N. D. Thureau, "Monte-carlo imaging for optical interferometry," in *Advances in Stellar Interferometry*, J. Monnier, M. Schöller, and W. Danchi, eds., *Proc. SPIE* **6268**, p. this volume, 2006.
7. E. Thiébaud, "Optimization issues in blind deconvolution algorithms," in *Astronomical Data Analysis II*, J.-L. Starck and F. D. Murtagh, eds., *Proc. SPIE* **4847**, pp. 174–183, SPIE Press, (Bellingham, WA), 2002.